Supplementary Material

FIRE

***Title*: "Application of model-free and model-based kinetic methods in evaluation of reactions complexity during thermo-oxidative degradation process: Case study of [4-(hydroxymethyl)phenoxymethyl] polystyrene resin"**

Authors: Bojan Janković[*] ([*]*Corresponding author*), Vladimir Dodevski, Filip Veljković, Marija Janković and Nebojša Manić

Corresponding author affiliation: University of Belgrade, Department of Physical Chemistry, "Vinča" Institute of Nuclear Sciences – National Institute of the Republic of Serbia, Mike Petrovića Alasa 12-14, P.O. Box 522, 11001 Belgrade, Serbia

∗ Supplementary Material content (S-1):

● Results content (*S-1-S-2*):

S.I. Chemical composition and properties of the resin used in the study

As testing system, *p*-alkoxybenzyl alcohol resin or [4-(hydroxymethyl)phenoxymethyl] polystyrene (Wang) resin was used. This resin is often used for solid phase side peptide synthesis, both in the research scale and in the production. Under the word "resin", there are two parts, namely: 1) the solid support, and 2) the spacer/linker. The main requirement of a solid support is to be chemically stable, throughout all conditions of the synthesis procedure. On the other hand, linker/spacer is a chemical entity that is permanently attached onto a polymer support, which temporarily links a growing peptide on current support. Large variety of linkers were developed, all of which are used in polystyrene (PS) core resins. So, the concept of Wang resin makes *p*-alkoxybenzyl alcohol linker (Wang linker) and polystyrene (PS) (polymer) solid support, which is shown in the **Scheme S1**.

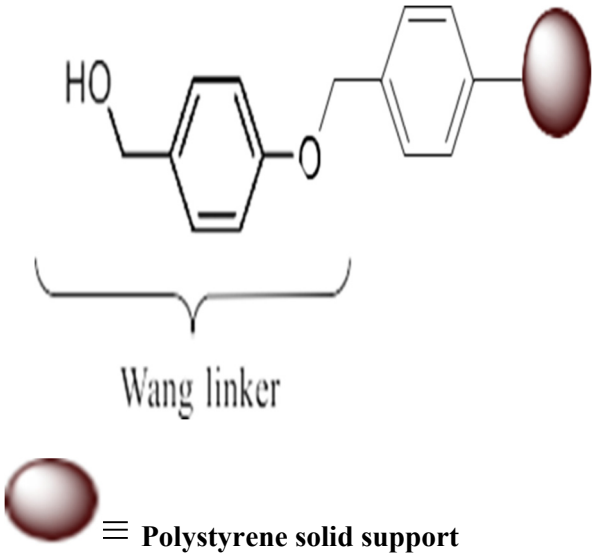

Scheme S1. The concept of the solid support with linker/spacer, which together form [4-(hydroxymethyl)phenoxymethyl] polystyrene resin (solid colored ball represents polystyrene (PS) solid support).

The Wang resin studied in this article, is commercial Merck (Merck & Co., Inc., Whitehouse station, New Jersey, USA) resin in a form of spherical beads (resin pearls) packed in 5 g glass bottle. The degree of 1% cross-linking offers the best compromise between mechanical stability and swelling properties. The resin belongs to chemical synthesis, solid supported synthesis and specialty synthesis related categories. The current resin belongs to the strong base anion-exchange resin, with a matrix consisted of polystyrene divinylbenzene (PS/DVB) copolymer, and hydroxide single bond OH group. More information about the resin used in this research is presented in the **Table S1**.

Table S1 Characteristics of [4-(hydroxymethyl)phenoxymethyl]polystyrene (4-benzyloxybenzyl alcohol) resin beads.

Resin brand	Resin description	Particle size (µm) [a]	Bead (PS) + Linker [b]	Extent of labeling
Merck	PS with 1 % (cross-linking) DVB	37 – 75 (200 – 400 mesh)	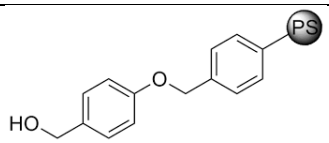	0.5 – 1.0 mmol·g^{-1} OH loading

[a] An narrow particle size distribution has a major advantage, as the homogeneous size of employed polymer particles is crucial for achieving uniform reaction conditions, throughout each individual resin bead.

[b] 4-hydroxybenzyl alcohol moiety (linker) (OH is the linking functional group) bound to a polystyrene (PS) core - polystyrene-based resin (linkage has good stability to a variety of reaction conditions, but can be readily cleaved by moderate treatment with an acid). The *p*-alkoxybenzyl linker (commonly known as Wang linker) is primarily used for the attachment of molecules possessing a free carboxyl group, but has been used to attach a range of functionalities (it can be converted to bromide, chloride, iodide, or trichloroacetimidate, which in tum can be displaced with various nucleophilic functional groups.

S.II. Characteristics process indices

The resin thermo-oxidative process indices, such as the ignition temperature (T_i), the temperature at the maximum of DTG (the temperature at the maximum mass loss rate) (T_p or T_{max}), the burnout temperature (T_b), the corresponding times (t_i, t_p and t_b), and the maximum and average DTG ($-R_p$, and $-R_v$) process rates (in %/min), can be derived from TG-DTG curves [1-3]. Beside these quantities, four other process performance indices, such as comprehensive combustibility (S), flammability index (C), the ignition index (D_i) and burnout index (D_b) can be calculated from Eqs. (S1) – (S4):

$$S = \frac{(-R_p)\cdot(-R_v)}{T_i^2 \cdot T_b} \tag{S1}$$

$$C = \frac{(-R_p)}{T_i^2} \tag{S2}$$

$$D_i = \frac{(-R_p)}{t_i \cdot t_p} \tag{S3}$$

$$D_b = \frac{(-R_p)}{\Delta t_{1/2} \cdot t_p \cdot t_b}, \tag{S4}$$

where $\Delta t_{1/2}$ represents the time range of $DTG/DTG_{(max)} = 0.5$ (min), while $DTG_{(max)}$ is the resin maximum process rate (%/min). More detailed instructions in determining the appropriate ignition and burnout characteristics of tested material, as well as the calculation method related to comprehensive thermo-oxidative properties can be found elsewhere [4]. Considering T_i, when the ignition temperature is low, it is easy igniting the tested material. The burnout of the material is the indicator to stand for its reaction degree. The higher the burnout, the fewer the combustible components left in the investigated material. The burnout temperature refers to the temperature at which the reaction system is almost completely consumed. The exact recognition of the burnout temperature for the resin, enables us to provide a useful insight into the operation of the resin in the process. Related to index S, when the S is higher, the combustion performance of the tested resin is in good condition. Additionally, the larger the flammability index (C), the better is "combustibility" of the resin. Likewise, if the ignition index (D_i) is larger, the better is the performance of the resin ignition. The index D_b is the important factor for characterizing the "combustibility" of *combustibles* in the present resin. The higher D_b value indicates on the good burnout performance of the tested resin, improving the *combustion performance* generally.

S.III. Kinetic analysis

The rate equation for a single-step solid-state degradation process under isothermal heating is given by the following equation:

$$\frac{d\alpha}{dt} = A \cdot exp\left(-\frac{E_a}{RT}\right) \cdot f(\alpha), \tag{S5}$$

where R is the universal gas constant (8.314 J/(mol·K)), A is the pre-exponential factor (1/s), E_a is the activation energy (J/mol), T is the absolute temperature (K), $f(\alpha)$ is the differential form of reaction model, while α is the conversion (the extent of reaction; dimensionless), expressed as $\alpha = (m_o - m)/(m_o - m_\infty)$, where m_o and m_∞ are

original (initial) and ultimate mass of the sample, respectively, and m is the actual mass of the sample at instantaneous temperature (T) and the time (t). Inserting the constant linear heating rate, $\beta = dT/dt$, into the Eq. (S5), will give the rate equation (Eq. (S6)) under the dynamic heating conditions, as:

$$\beta \cdot \frac{d\alpha}{dT} \equiv \frac{d\alpha}{dt} = A \cdot exp\left(-\frac{E_a}{RT}\right) \cdot f(\alpha). \tag{S6}$$

The parameters A, E_a and $f(\alpha)$ represent the kinetic triplet, which are to be determined during the kinetic analysis of investigated process.

The integral dependence for solving the Eq. (S6) leads to integration of Arrhenius equation giving:

$$g(\alpha) = \int_0^{\alpha} \frac{d\alpha}{f(\alpha)} = \frac{A_\alpha}{\beta} \int_0^{T_\alpha} exp\left(-\frac{E_{a,\alpha}}{RT_\alpha}\right) dT_\alpha \cong \frac{A_\alpha}{\beta} \cdot J(E_{a,\alpha}, T_\alpha), \tag{S7}$$

where $g(\alpha)$ is the integral form of $f(\alpha)$, $J(E_{a,\alpha},T_\alpha)$ is the temperature integral, while T_α, A_α and $E_{a,\alpha}$ represent the temperature at given conversion (α), the pre-exponential factor and the activation energy values at considered conversion (α), respectively. Since $f(\alpha)$ is independent of the temperature and heating rate, this is likewise for its integral term. Note that the derivation of the above equation involves an assumption that the E_a must be a constant with respect to conversion; the temperature integral $J(E_{a,\alpha},T_\alpha)$ has no analytical solution, but many approximations exist with the aim of solving this integral, through approximated procedures [5-7].

S.III.1. Model-free analysis: Friedman (FR), Vyazovkin (VY) and Numerical (NM) methods

Friedman (FR) isoconversional approach [8] relies on a differential solution of the Eq. (S6), with assumption that the chemistry of the degradation process depends only on the rate of mass loss and is independent from the temperature. Friedman relation can be derived by taking logarithms of both sides of the Eq. (S6) under different heating rates, such as:

$$log\left(\frac{d\alpha}{dt}\right)_{\alpha,i} = log[A_\alpha \cdot f(\alpha)]_i - \frac{E_{a,\alpha}}{RT_{\alpha,i}}. \tag{S8}$$

where subscript "i" designates i-th value of the used heating rate (β_i), while $T_{\alpha,i}$ represents the temperature at which the given conversion (α) is reached, at the corresponding heating rate, β_i. The activation energy ($E_{a,\alpha}$) at $\alpha = const.$, can be determined from the slope of the isoconversional line at a given value of α. The linear plot of $log(d\alpha/dt)_{\alpha,i}$ against $1/T_{\alpha,i}$ is generated for different heating rates, and the activation energy is determined from: $slope \equiv -E_{a,\alpha}/R$. When used derivative conversion data, this makes that the differential isoconversional method can prone to noise sensitivity and numerical instability, but modern software's contain very effective filters for removing noise and background difficulties, thus obtaining reliable data and facilitating their interpretation.

Vyazovkin (VY) advanced method uses the non-linear regression proposed by Senum and Yang, which makes it more accurate over a wider range of TG data [9], and circumvents the inaccuracies related to analytical approximation of the temperature integral. However, its application remains limited as the mass transfer becomes limiting, at very high conversions (above $\alpha = 0.75/0.80$ (= 75 %/80 %)). The advanced Vyazovkin's (VY) model-free method is a widely recommended integral isoconversional approach, for the accurate determination of activation energies, E_a's [10]. This method proposes an exact equation (non-linear) based on general assumption,

that the reaction (kinetic) model is independent on the heating rate. The activation energy at a specific conversion value, α, is obtained by determining the E_a value, which minimizes the Eq. (S9):

$$\sum_{i=1}^{n}\sum_{j\neq i}^{n}\frac{I(E_{a,\alpha},T_{\alpha,i})\cdot\beta_j}{I(E_{a,\alpha},T_{\alpha,j})\cdot\beta_i}=min. \tag{S9}$$

where

$$I(E_{a,\alpha},T_\alpha)=\int_0^{T_\alpha}e^{-\frac{E_{a,\alpha}}{RT}}dT. \tag{S10}$$

In above equations, $E_{a,\alpha}$ and T_α are the activation energy and the temperature at a conversion α, respectivelly, obtained from independent experimental runs *i* and *j*, and performed at different heating rates, *β*'s. The integral is numerically evaluated by using the trapezoidal rule and a uniform grid spacing, that is continuaslly decreased, until a difference in the integral values is smaller than 10^{-6}, between the consecutive interactions, is obtained. Different activation energy values are then used in above equations and, the activation energy for the process, determined as the value of $E_{a,\alpha}$, which gives the lower result, for above, Eq. (S9). Advantages of this method are that it can be used for multi-step reactions, and that all reaction points are assessed. Disadvantages of this method are that it is only suitable for dynamic (non-isothermal) measurements, and that, it provides average values of E_a for both parallel and independent reactions. The method described above represents an incremental integral isoconversional method, where the specified conversion range Δα is very narrow, with a step of Δα = 0.01. For simplicity in the text, the method is denoted by "VY".

Numerical optimization method represents model-free method using non-linear least square optimization. This method was developed by NETZSCH Co., and it is implemented in the Kinetics Neo software. Numerical method searches the optimal functions $E_a(\alpha)$ and $logA(\alpha)$ in order to get best fit for the conversion (T, t). Numerical method is based on the results of the analytical Friedman's method (it is called often modified Friedman's method). The results of Friedman method (curves $E_a(\alpha)$ and $A(\alpha)$) are optimized numerically in order to achieve the better fit between experimental and simulated curves. Calculation of $logA$ is implemented for the first order reaction, $f(\alpha) = 1 - \alpha$. The function for optimization is the sum of squares of deviations between measured value *Conversion_experimental* (T) and calculated value *Conversion_simulated* (T). This sum is calculated over all curves and over all points in each curve, such as:

$$\Omega=\sum_{Curves}\sum_{Points}\left[\alpha(T)_i^{calc}-\alpha(T)_i^{exp}\right]^2, \tag{S11}$$

where $\alpha(T)_i^{calc}$ and $\alpha(T)_i^{exp}$ represent calculated and experimental conversion values (this also can be implemented on the TGA-signals) for considered *i*-th heating rate used. The numerical method searches numerically values $E_a(\alpha)$ and $logA(\alpha)$ which minimize the optimization function Ω (Eq. (S11)). Internally, each point of curves $E_a(\alpha)$ and $A(\alpha)$ is a subject of the small changes, and for each change, the sum of the squares of residuals is checked: is it better or worse than before. If better then new point in $E_a(\alpha)$ or $A(\alpha)$, is saved. The iterations are repeated until no any numerical improvements happens. Advantage of numerical optimization is reflected in the fact that can be applied for multiple-step reactions with evaluation of each reaction point at various heating rates, where the mean values of kinetic parameters may be extracted.

For all presented kinetic calculations, software Kinetics Neo (Product version: 2.6.6.7) was used. This software is used most often ability to transform "*ln*" scale into the "*log*" scale data, where normally operates, especially in the case of Friedman's method data processing. For all above methods (FR, VY and Numerical (NM)), the software uses two available approaches in finding an logarithm of pre-exponential factor (*logA*): a) *logA* can be estimated from intercept of Eq. (S8) (Friedman method) and following mathematical relations for other two methods, on a similar principle as for determination of E_a, for known or assumed $f(\alpha)$ (usually first-order kinetics), and b) *logA* can be found from the application of kinetic compensation effect (KCE) model [11-15].

Summarizing these isoconversional (model-free) methods, the model-free analysis contains five main assumptions, namely: 1) it is based *only* on the *one kinetic equation*, as:

$$\frac{d\alpha}{dt} = A(\alpha) \cdot f(\alpha) \cdot exp\left[-\frac{E_a(\alpha)}{RT}\right], \quad \text{(S12)}$$

where $A(\alpha)$ and $E_a(\alpha)$ are the conversion-dependent pre-exponential factor (1/s) and the conversion-dependent activation energy (J/mol), which represent wanted quantities in the model-free kinetic analysis ($A(\alpha)$ can be found only with assumption of the function $f(\alpha)$); 2) E_a and A *depend on* α, 3) *the reaction rate* at the same conversion is only a *function of temperature*, 4) the total effect (total mass loss or total peak area) must be *the same for all curves* (TGA-signals), and 5) *changes* of the mechanism should be at *the same conversion value*. Considering applied model-free methods, kinetic parameters are determined using the points at the same conversion between α = 0.01 (= 1 %) to α = 0.99 (= 99 %) with a conversion step increment of Δα = 0.01, from measurements at four different heating rates (β = 5, 10, 20 and 30 K/min).

S.III.2. Model-based analysis

Model-based kinetic analysis represents the procedure for the complex chemical process consisting of individual reaction steps, where each step can be individually connected to another reaction steps (consecutive, competitive, independent, etc.), in order to build a kinetic model of the complex process under the investigation. Model-based kinetic approach describes the reaction rate of multi-step chemical reactions by the system (or the set) of kinetic equations, where each reaction step has own kinetic equation and own kinetic triplet, containing activation energy (E), pre-exponential factor A, as well as the reaction type (Table S2).

Table S2 Reaction models used for solid-state kinetics evaluations studied in this work, within Kinetics Neo software. The rate expression: $de/dt = k(T) \cdot f(e,p)$ ($k(T)$: Arrhenius type temperature-dependent rate constant, $f(e,p)$: the reaction model; e - the starting concentration of the reactant (e = 1 - α), p - the concentration of the final product (p = α (conversion))).

Model code	$f(e,p)$ [a]	$f(\alpha)$ [b]	**Reaction type**
F1	e	(1 - α)	First order
F2	e^2	$(1 - \alpha)^2$	Second order

F*n*	e^n	$(1 - \alpha)^n$	*n*-th order
D1	$0.5/(1 - e)$	$1/2\alpha$	One-dimensional diffusion
D2	$-1/\ln(e)$	$1/[- \ln(1 - \alpha)]$	Two-dimensional diffusion
D3	$1.5e^{1/3}/(e^{-1/3} - 1)$	$(3/2)(1 - \alpha)^{2/3}/[1 - (1 - \alpha)^{1/3}]$	Jander three-dimensional diffusion
D4	$1.5/(e^{-1/3} - 1)$	$(3/2)/[(1 - \alpha)^{-1/3} - 1]$	Ginstling–Brounshtein three-dimensional diffusion
R2	$2e^{1/2}$	$2\cdot(1 - \alpha)^{1/2}$	Reaction on the two-dimensional interface
R3	$3e^{2/3}$	$3\cdot(1 - \alpha)^{2/3}$	Reaction on the three-dimensional interface
B1	$e\cdot p$	$(1 - \alpha)\cdot\alpha$	Autocatalysis according to the Prout–Tompkins equation
B*na*	$e^n p^a$	$(1 - \alpha)^n\cdot\alpha^a$	*n*-th order autocatalysis according to the Prout–Tompkins equation
C1-X (C1)	$e(1 + K_{cat}X)$	$(1 + k_{cat}\cdot\alpha)(1 - \alpha)$	First-order autocatalysis, X is the product in a complex model, often X = *p*
C*n*-X (C*n*)	$e^n(1 + K_{cat}X)$	$(1 + k_{cat}\cdot\alpha)(1 - \alpha)^n$	Reaction of *n*-th order with autocatalysis by product
C*nm*	$e^n(1 + K_{cat}X^m)$	$(1 + k_{cat}\cdot\alpha^m)(1 - \alpha)^n$	Reaction of *n*-th order with *m*-power autocatalysis by product
A2	$2e(-\ln(e))^{1/2}$	$2\cdot(1 - \alpha)[- \ln(1 - \alpha)]^{1/2}$	Two-dimensional nucleation (Avrami–Erofeev)
A3	$3e(-\ln(e))^{2/3}$	$3\cdot(1 - \alpha)[- \ln(1 - \alpha)]^{2/3}$	Three-dimensional nucleation (Avrami–Erofeev)
A*n*	$n\cdot e(-\ln(e))^{(n-1)/n}$	$n\cdot(1 - \alpha)[- \ln(1 - \alpha)]^{1-1/n}$	*n*-dimensional nucleation (Avrami–Erofeev)

[a] According to Eq. (S13).

[b] According to Eq. (S6).

Result of this analysis represents the kinetic model with kinetic parameters for each reaction step considered. Kinetic parameters can be found from the best fit of kinetic model for actual experimental data. Model-based analysis has the ability to display the reaction rate for each step and concentration of each reactant. This approach includes three main assumptions, which are as follows: *a*) the reaction rate for individual reaction steps can be described by the Eq. (S13):

$$\frac{de_j}{dt} = A_j \cdot f_j(e_j, p_j) \cdot exp\left(-\frac{E_j}{RT}\right), \quad \text{(S13)}$$

where $f_j(e_j,p_j)$ represents the function of reaction type (Table S2), e_j is the initial reactant concentration, p_j is the product concentration, A_j and E_j are the pre-exponential factor and the activation energy, related only for the specific reaction step, while j represents the number of specific reaction steps; *b*) all kinetic triplets are assumed to be constant during the reaction advancement, for every individual reaction step, and *c*) total thermo-analytical signal is the sum of signals of the individual reaction steps – the signal of each step is calculated as the reaction rate multiplied by the total effect of the given step, e.g., the total enthalpy change or the total mass loss, specified by the following equation:

$$m = m_o - \Delta m \cdot \left[\sum_{j=1}^{n} Contribution_j \int \left(\frac{d(e_j \rightarrow p_j)}{dt}\right)_j dt\right] \quad \text{(S14)}$$

where m is the mass, m_o is the initial mass, Δm is the total mass change, $(e_j \rightarrow p_j)$ represents the heat flow on the path from the reactant "e" to the product "p", while "$Contribution_j$" corresponds to the contribution of the j-th reaction step to the overall heat flow. Kinetic Neo software within the package that contains model-based analysis has the ability to add kinetic models as *per* their physical and chemical reactions of the materials, whether it is a competitive step (parallel/split reaction) or a consecutive step (series reactions). For each reaction step, it is possible to add the reaction types in order to determine kinetic triplets, as well as to optimize each reaction step with experimental results. After optimizing each reaction step, the customer can optimize the constructed model towards the entire process, for the kinetic triplets, as well as for the predictions [16]. The actual analysis uses non-linear regression methods and allows the optimization of parameters for individual steps or for complete model. The fit results act as the agreement between the experimental and simulated curves, for: the measurement output – signals, conversion, the conversion rate, concentration for each reactant (and of all reactants), and the reaction rates for all steps.

S.IV. Preliminary determination of the type of reaction models involved in the resin degradation mechanism

Based on the conducted model-free (isoconversional) analysis, the appropriate Friedman's (FR) isoconversional plots (for the conversion step of 0.01) were created, and these plots are presented in Fig. S4.

From the Friedman's (FR) analysis presented in Fig. S4, on the basis of isoconversional line inclination angle to ordinate axis, the arguable reaction type can be decrypted. Obviously, based on the looks of entire Friedman's analysis plots, the considered combustion process is obvious multi-stepped. Two clearly peaks are discernible at the considered heating rates, the first one is positioned at lower conversions, while the second one is positioned at high conversions. From the isoconversional lines (shades of "pink" to "blue" lines to the particular conversion value), the peak slope is much steeper than isoconversional lines, which suggests on the presence of accelerated reaction (the process is accelerating). The presence of accelerated reaction(s) can be detected based on the fact that the slope of isoconversional lines is gentler than the first peak slope on the Friedman's plots (Fig. S5). Also, it can be observed that exists a slope of experimental values, which is lower than the slope of Friedman's isoconversional lines (Figs. S4 and S5), suggesting on the presence of the reaction with deaccelerating character (such as diffusion models, contracting geometry, the n-th order reaction models) [17]. The existence of clear, the

second peak at all heating rates at Friedman's plots (Figs. S4 and S5), is an indication about the completion of thermo-oxidative degradation at profiled ultimate temperature. It was observed that distances between the constant conversion points are increasing with a heating rate (except, when moving from β = 20 K/min to β = 30 K/min), indicating the acceleration of the process. But, it was also observed, that there is a decreasing of this distance in the portion(s) of the process near and at, where the second peak is situated (Figs. S4 and S5), depending on heating rate applied (as deaccelerating character of the process). All this information can be useful during the selection of the best reaction models, in the case of a complex kinetic scheme of degradation process (related to model-based kinetic analysis).

S.V. Kinetic analysis related to determination of the rate-controlling steps in the resin degradation process

The behavior of reaction rates in complex degradation mechanism, which includes a mixture of various reaction steps, as consecutive and single-step reactions, largely determine the rate constants of individual steps. Therefore, their more detailed analysis can determine which step has a decisive role in the entire process (in terms of the formation of desired products), taking into account the influence of the heating rate. Of course, this is conditional for concentration variation of each reactant and product, considering the whole set of kinetic equations. Fig. S6 a) – d) shows the rate constants against temperature, for each elementary step in hx:, model (see the main text), including autocatalytic fractions for models based on catalysis, with k-values obtained for heating rates of β = 5 K/min (low) and β = 30 K/min (high).

As can be seen from Fig. S6, for all reaction steps, the rate constant exhibits increasing trend with temperature, but $k(T)$ dependency varies from the linear to exponential shape, depending on the reaction type and "frequency" magnitude. Also, it can be seen that $k(T)$ plots differ in their slopes, which depend on the value of activation energies. Considering values of rate constants at different heating rates (5 K/min and 30 K/min), there are differences for certain reaction steps, which as the fact, emphasizes the influence of the heating rate (β). It is especially important whether they take place through the absorption or the release of heat.

Fig. S7 a) and b) shows the mean values of rate constants regarding to each reaction step in hx:, model, at 5 K/min and 30 K/min, respectively. If we consider consecutive reactions steps $A \overset{k_1}{\rightarrow} B \overset{k_2}{\rightarrow} C$ at low β's (5 K/min) (Fig. S7 a)), $k_1 >> k_2$, so in this considered case, the following approximated equation holds, such as: $c \approx (1/a_o^{n-1})\cdot exp(-k_2\cdot t)]$ (c is the concentration of the product, while a_o represents the reactant initial concentration, and n is the reaction order). Therefore, the elementary step $B \rightarrow C$ (the second reaction) is the rate-controlling step, for the observed segment of degradation process. This step was described by kinetic model Cnm, which exhibits an autocatalytic nature. Thus, the actual step proceeds as global reaction step, which is, in turn, comprised of two parallel reactions, namely, the n-th order process, and an m-th order autocatalytic reaction. The *first one* represents the formation of benzaldehyde from benzyl alcohol moiety of Wang linker, while the *second one* represents an oxidation of benzaldehyde to benzoic acid (see the main text). The effective rate constant for this global reaction depends on the ratio of rate constants of these parallel reactions. This ratio was found to be $k_{eff} = k_{n\text{-th}}/k_{autocat.} \sim 4.7 \times 10^{11}$. The latter suggests that benzaldehyde is strongly favoring in this rate-determining step, compared to

benzoic acid. Its contribution to the overall process is high and it was characterized by an exothermic effect (see discussion in the main text). It should be noted that similar situation holds for the high heating rate (Fig. S7 b)). But for the application to a large-scale in a chemical reactor, the use of lowest possible heating rates is strongly recommended, in order to better control the degradation process of the resin (see discussion in the main text). It should be noted that intermediate is not the part of the rate equation, so, the above case, corresponds to the situation that we have one uni-molecular reaction and one bi-molecular reaction.

As for the second sequential mechanism within hx:, model, i.e., considering consecutive reactions steps $D \overset{k_1^*}{\rightarrow} E \overset{k_2^*}{\rightarrow} F$, at low β's (5 K/min) (Fig. S7 a)), $k_2^* >> k_1^*$, so in this case, it can be approximated an following equation: $f \approx d_o \cdot exp(-k_1^* \cdot t)$ (f is the concentration of the product, and d_o is the reactant initial concentration). So, in the observed reaction process segment, the rate-determining step represents transports of reactants to where they can interact and form the product, and therefore, at the low heating rate, above sequence can be approximated as $D \rightarrow F$ representing an apparent step, where the cage radicals (see the main text) directly generate gaseous products, without de-propagation reaction (intermediate step) (refer back to the discussion in the main text). So, at low heating rates, this goes like the single-step reaction.

However, at high heating rate values (Fig. S7 b)), we have a different situation. Here, it is that $k_2^* > k_1^*$. In the considered case, de-propagation reaction cannot be ignored, and the actual process stage performs as two-step consecutive reaction stage $D \rightarrow E \rightarrow F$. Accordingly, the high heating rates lead to the "complication" of this part of resin degradation process (here, specie(s) E are not so desired products). Thus, from the point of view of chemical engineering, the use of low heating rates is recommended, for easier extraction of gaseous products.

Among independent single-step reactions (steps $I \rightarrow J$ and $G \rightarrow H$), it is an obvious that the reaction $G \rightarrow H$ controls accumulated fuels consumption, where the large amount of heat is released, but it is very sensitive to a changes in the heating rate (Fig. S7). Considering results present in Fig. S7 a) and b), it is evident that higher heating rates (~ 30 K/min) significantly accelerate the reaction $G \rightarrow H$. For this case, as an important point seems the determination a critical rate of the temperature rise, within autocatalytic oxidation reaction. These are issues about authors discuss in the sub-section *3.3.2.6.* (within the main text), and which were present in a mechanistic decryption of the process by using the model-free methods. Namely, these conditions correspond to those for experiments in Accelerating Rate Calorimeter (ARC). Therefore, this analysis can serve researchers for a positive way of thinking, regarding investigation of oxidative reactions for this type of resin.

S.VI. Safety analysis – characterization of runaway reactions and use of kinetic data in adiabatic simulations (Adiabatic 24 prediction)

The precise prediction of reaction progresses in adiabatic conditions is necessary for the safety analysis of many technological processes [18-23]. Calculations of an adiabatic temperature-time curve for the reaction progress can also be used to determine the decrease of thermal stability of materials during storage, at temperatures near the threshold temperature for triggering the reaction. Due to insufficient thermal convection and limited thermal conductivity, a progressive temperature increase in the sample can easily take place, resulting in hazard situation. Because degradation reactions usually have a multi-step nature, the accurate determination of the kinetic

characteristics strongly influences the ability to correctly describe the progress of process. The use of simplified kinetic models for the assessment of runaway reactions can, on one hand, lead to economic drawbacks, since they result in exaggerated safety margins. On the other hand, it can cause the dangerous situations, when the heat accumulation is underestimated. For adiabatic self-heating reactions, incorrect kinetic description of the process is usually the main source of prediction errors. The kinetics based approach for determination of the time to maximum rate under adiabatic conditions can be seen elsewhere [24].

An important problem with adiabatic data is the uncertainty of the reactant state at the onset temperature of the adiabatic mode. The problem originates from the simple facts that it is just impossible to maintain adiabatic conditions from the beginning of an experiment and the sensitivity of an adiabatic calorimeter is limited. It is common practice to apply one or another type of thermal initiation. The adiabatic mode is established when a calorimeter first detects heat generation by the reaction. Usually, it is assumed that due to high sensitivity of the calorimeter, the conversion at the detected onset temperature is negligible (*apropos* "zero" assumption), although, it is evident that reaction started before the onset and conversion is non-zero, but there is no way to determine it directly. Nevertheless, it turns out that even very small but non-zero conversion strongly affects the reaction course and kinetics evaluated under "zero" assumption, may be unsafe or even wrong. Consequently, this description is strongly grounded on the fact that the established complex kinetic mechanism (determined by the model-based approach) contains reactions described by *n*-th order reaction and autocatalytic reaction. Formulation of adiabatic problem in the actual simulation that operates through the Kinetic Neo software prediction tool was based on the concept presented by Kossoy et al. [25]. In this work, DSC measurements or other calorimetry testing procedures were not directly implemented, but a given software is capable of simulating the process in the described reaction (adiabatic) conditions, based on the reported kinetic results using both, model-free and model-based methods, respectively. So in that sense, an experimental data cannot be directly used to calculate the time for the reaction and the adiabatic temperature rise. The experimental data must be corrected for the effect of the vessel's heat capacity using the *phi* factor (ϕ). There are several methods of correcting for the *phi* available in the literature. The most straightforward is to correct the measured adiabatic temperature rise by the following:

$$(\Delta T_{ad})_{actual(real)} = \phi(\Delta T_{ad})_{measured}, \tag{S15}$$

and the time for the reaction by

$$t_{actual(real)} = \frac{t_{measured}}{\phi}. \tag{S16}$$

Alternative methods of correcting for *phi* factor given in the literature are the method by Fisher presented in the DIERS project manual [26] and that by Huff [27]. All these methods can be compared with an ideal case. The ideal case was generated from thermo-analytical data by the kinetics results, such that, when the simulation model was run with relevant *phi* factor, the simulation model reproduced exactly the experimental curve. Having exactly matched the experimental data with the simulation curve, the simulation model was then run with $\phi = 1$ (the lower is the influence of the container, and the more representative the result is of the sample itself). Sensitivity analysis related to time to runaway includes important physical data, such as pre-exponential factor, activation energy, heat capacity and start (initial) temperature for the reaction, and they can be accurately determined based on the

obtained models, used in the simulation program. So that, for the achievement of the adiabatic conditions leads to the following equation:

$$\frac{dT}{dt} = \frac{1}{\phi} \cdot \Delta T_{ad,real} \cdot \left(\frac{d\alpha}{dt}\right), \tag{S17}$$

where dT/dt is the self-heat rate corresponding to T, $\Delta T_{ad,real}$ is the adiabatic temperature rise expressed as $\Delta T_{ad,real} = \Delta H/c_p$ (where ΔH is the enthalpy (J·g^{-1}) and c_p is the heat capacity of the material (J·g^{-1}·K^{-1})), while (dα/dt) represents kinetic expression described by the Eq. (S12) in the case of isoconversional analysis, i.e., described by Eq. (S13), in the case of model-based analysis. One can now use the kinetic based approach for prediction of the reaction progress $\alpha(t)$ and the rate dα/dt as well as the development of the temperatures $T(t)$ and dT/dt and adiabatic induction times, at any selected starting temperatures. It should be noted that the ϕ factor influences the simulation of the process in Accelerating Rate Calorimeter (ARC) experiment, so, the ϕ factor influences on the following:

a) $\Delta T_{ad,measured}$, because it comes from above description that $\Delta T_{ad,measured} = (1/\phi)\cdot\Delta T_{ad,real}$, and
b) Time to maximum rate (TMR) (the time from the beginning of an adiabatic process to the maximum reaction rate), in a different level depending on the type of decomposition kinetics. TMR as an important index for chemical process safety, can be approximately calculated from the expression: TMR $\approx R\cdot T^2/E\cdot$(d$T$/d$t$), where R is the universal gas constant, T is the temperature denoted at exothermic peak area, E is the activation energy value, determined for the reaction step where exothermic event occurs, while (dT/dt) is given by the Eq. (S17).

The ϕ factor (thermal inertia factor) represents the ratio of the heat capacity of the material and the vessel to the heat capacity of the material c_p. For the absence of the container, $\phi = 1$. So, the thermal Inertia (ϕ factor) can be presented by the following expression:

$$\phi = 1 + \frac{(Mass \times Specific\ heat\ capacity)_{Container}}{(Mass \times Specific\ heat\ capacity)_{Sample}}. \tag{S18}$$

Therefore, when the ϕ factor is close or equal to the unity, this represents a strict adiabatic conditions.

For the complex reactions, the complete kinetic model comprising heat balance equation and energy source equation, which are integrated numerically within the Kinetics Neo software prediction tool, resulting in the $T(t)$ response or in the $\alpha(t)$ response. Likewise, the software enables direct estimation of TMR (under adiabatic condition) and T_{D24} quantity, where the latter represents the temperature at which the time to maximum rate of the runaway reaction is 24 hours (in other words, T_{D24} means that an intervention is possible within 24 hours).

Considering industrial scale-up process, the knowledge of the enthalpy value alone is not always enough for a safe chemical process. If cooling fails [28], the continuing reaction will increase the temperature in the reactor until the reactants are consumed. Then, the reaction and corresponding self-heating will have finished and the final theoretical temperatures will be achieved. This temperature is called maximum temperature of synthesis reaction (MTSR). Safety of industrial processes depends on how high the MTSR is. If it is too high, it can initialize a secondary process with further self-heating. This secondary reaction is usually some degradation reaction, which is exothermal in its nature, and may leads to a further temperature increase. In fact, if the rapid secondary reaction is initialized, the risk of runaway and thermal hazard is very high. If the value of MTSR is lower than T_{D24}, this means that after finishing the primary reaction, the rapid secondary reaction is not initialized, and the risk of

runaway reaction is a very low. If the MTSR is higher than T_{D24}, the secondary reaction starts already during the primary reaction, and it is impossible to avoid the runaway, with the dangerous consequences. So, knowing T_{D24}, the maximum allowable temperature for the process of the interest can be derived. Based on the value of reaction enthalpy, it is possible to evaluate the type of reactor that would be constructed, bearing in mind that Eq. (S17) is completely valid for large-scale experiments, where tons-scale of starting material (resin) is applied.

References

1. Chen, R.; Li, Q.; Xu, X.; Zhang, D.; Hao, R. Combustion characteristics, kinetics and thermodynamics of *Pinus Sylvestris* pine needle via non-isothermal thermogravimetry coupled with model-free and model-fitting methods. *Case Stud. Therm. Eng.* **2020**, *22*, 100756. https://doi.org/10.1016/j.csite.2020.100756

2. Tang, L.; Xiao, J.; Mao, Q.; Zhang, Z. et al. Thermogravimetric analysis of the combustion characteristics and combustion kinetics of coals subjected to different chemical demineralization processes. *ACS Omega* **2022**, *7(16)*, 13998-14008. https://doi.org/10.1021/acsomega.2c00522

3. Diao, R.; Lu, H.; Yang, Y.; Bai, J.; Zhu, X. Comparative insights into flue gas-to-ash characteristics on co-combustion of walnut shell and bio-oil distillation sludge under atmospheric and oxy-fuel condition. *Comb. Flame* **2022**, *246*, 112383. https://doi.org/10.1016/j.combustflame.2022.112383

4. Jia, G. Combustion characteristics and kinetic analysis of biomass pellet fuel using thermogravimetric analysis. *Processes* **2021**, *9*, 868. https://doi.org/10.3390/pr9050868

5. Doyle, C. Kinetic analysis of thermogravimetric data. *J. Appl. Polym. Sci.* **1961**, *5(15)*, 285-292. https://doi.org/10.1002/app.1961.070051506

6. Senum, G.I.; Yang, R.T. Rational approximations of the integral of the Arrhenius function. *J. Therm. Anal. Calorim.* **1977**, *11(3)*, 445-447. https://doi.org/10.1007/BF01903696

7. Wanjun, T.; Yuwen, L.; Hen, Z.; Zhiyong, W.; Cunxin, W. New temperature integral approximate formula for non-isothermal kinetic analysis. *J. Therm. Anal. Calorim.* **2003**, *74*, 309-315. https://doi.org/10.1023/A:1026310710529

8. Friedman, H.L. Kinetics of thermal degradation of char-forming plastics from thermogravimetry. Application to a phenolic plastic. *J. Polym. Sci. Part C Polym. Symp.* **1964**, *6(1)*, 183-195. https://doi.org/10.1002/polc.5070060121

9. Pérez-Maqueda, L.A.; Criado, J. The accuracy of Senum and Yang's approximations to the Arrhenius integral. *J. Therm. Anal. Calorim.* **2000**, *60*, 909-915. https://doi.org/10.1023/A:1010115926340

10. Vyazovkin, S. Evaluation of activation energy of thermally stimulated solid-state reactions under arbitrary variation of temperature. *J. Comput. Chem.* **1997**, *18(3)*, 393-402. https://doi.org/10.1002/(SICI)1096-987X

11. Sbirrazzuoli, N. Determination of pre-exponential factor and reaction mechanism in a model-free way. *Thermochim. Acta* **2020**, *691*, 178707. https://doi.org/10.1016/j.tca.2020.178707

12. Liavitskaya, T.; Vyazovkin, S. All you need to know about the kinetics of thermally stimulated reactions occurring on cooling. *Molecules* **2019**, *24(10)*, 1918. https://doi.org/10.3390/molecules24101918

13. Das, P.; Tiwari, P. Thermal degradation kinetics of plastics and model selection. *Thermochim. Acta* **2017**, *654*, 191-202. DOI:10.1016/j.tca.2017.06.001

14. Vyazovkin, S. Determining preexponential factor in model-free kinetic methods: How and why? *Molecules* **2021**, *26*, 3077. https://doi.org/10.3390/molecules26113077

15. Choudhary, J.; Alawa, B.; Chakma, S. Insight into the kinetics and thermodynamic analyses of co-pyrolysis using advanced isoconversional method and thermogravimetric analysis: A multi-model study of optimization for enhanced fuel properties. *Process Saf. Environ. Prot.* **2023**, *173*, 507-528. https://doi.org/10.1016/j.psep.2023.03.033

16. Moukhina, E. Comparison of isothermal predictions based on model-free and model-based kinetic methods. *J. Test. Eval.* **2014**, *42(6)*, 1377-1386. DOI:10.1520/JTE20140145

17. Sobek, S.; Werle, S. Solar pyrolysis of waste biomass: Part 2 kinetic modeling and methodology of the determination of the kinetic parameters for solar pyrolysis of sewage sludge. *Renew. Energy* **2020**, *153*, 962-974. https://doi.org/10.1016/j.renene.2020.02.061

18. Roduit, B.; Borgeat, Ch.; Berger, B.; Folly, P. et al. Advanced kinetic tools for the evaluation of decomposition reactions − Determination of thermal stability of energetic materials. *J. Therm. Anal. Calorim.* **2005**, *80*, 229-236. https://doi.org/10.1007/s10973-005-0641-6

19. Ticmanis, U.; Pantel, G.; Wilker, S.; Kaiser, M. *Precision required for parameters in thermal safety simulations*. 32nd International Annual Conference of ICT July, 2001, p. 135.

20. Folly, P. Thermal stability of explosives. *Chimia* **2004**, *58*, 394. doi:10.2533/000942904777677759

21. Pastré, J.; Wörsdörfer, U.; Keller, A.; Hungerbühler, K. Comparison of different methods for estimating TMR_{ad} from dynamic DSC measurements with ADT 24 values obtained from adiabatic Dewar experiments. *J. Loss Prev. Process Ind.* **2000**, *13*, 7-17. https://doi.org/10.1016/S0950-4230(99)00061-3

22. Frank-Kamenetskii, D.A. *Diffusion and Heat Transfer in Chemical Kinetics*, Plenum Press, New York, London, UK, 1969, pp. 35-48.

23. Dien, J.M.; Fierz, H.; Stoessel, F.; Killé, G. The thermal risk of autocatalytic decompositions: A kinetic study. *Chimia* **1994**, *48*, 542-550. DOI: https://doi.org/10.2533/chimia.1994.542

24. Roduit, B. *Advanced kinetics-based simulation method for determination of the thermal aging, thermal runaway TMR_{ad} and SADT using DSC*, Analysis Report (example) (The AKTS AG Advanced Kinetics and Technology Solutions, http://www.akts.com), June 11th, 2008, pp. 22-29.

25. Kossoy, A.; Misharev, P.; Belochvostov, V. *Peculiarities of Calorimetric Data Processing for Kinetics Evaluation in Reaction Hazard Assessment*. Conference: 53rd Annual Calorimetry Conference, Midland, Michigan, USA, August 9-14, 1998, pp. 1-9.

26. Fisher, H.G.; Forrest, H.S.; Grossel, S.S. et al. *Emergency Relief System Design Using DIERS Technology: The Design Institute for Emergency Relief Systems (DIERS) Project Manual*, John Wiley & Sons, Inc., Publication, New York, NY, USA, 1993 (ISBN: 978-0-816-90568-3), pp. 1-488.

27. Huff, J.E. Emergency venting requirements. *Plant/Oper. Prog.* **1982**, *1*, 211-229. https://doi.org/10.1002/prsb.720010405

28. Gygax, R. Chemical reaction engineering for safety. *Chem. Eng. Sci.* **1988**, *43*, 1759-1771. https://doi.org/10.1016/0009-2509(88)87040-4

Results:

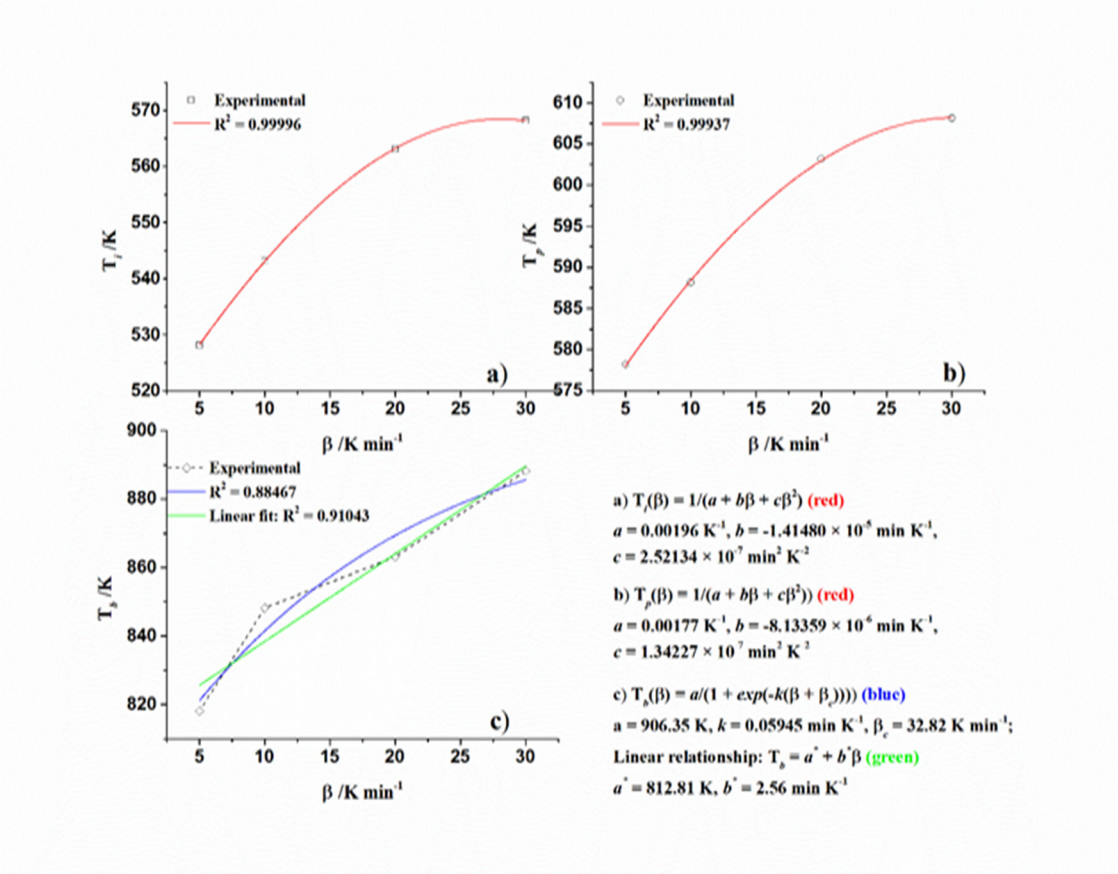

Figure S1. Thermal stability results related to [4-(hydroxymethyl)phenoxymethyl] polystyrene resin thermo-oxidative degradation process: **a)** Fitting applied to evolution of T_i values with β's, **b)** Fitting applied to evolution of T_p values with β's, and **c)** Fittings applied to possible evaluations of T_b values with β's. For each observed case, appropriate rational power relationship (**a)** and **b)**) and exponential relationship, with additional linear relationship (**c)**), were shown on the same graph (the corresponding values of parameters of the fitting are also indicated) [the *dashed line* under the case **c)** shows '*irregular*' trend of experimental points].

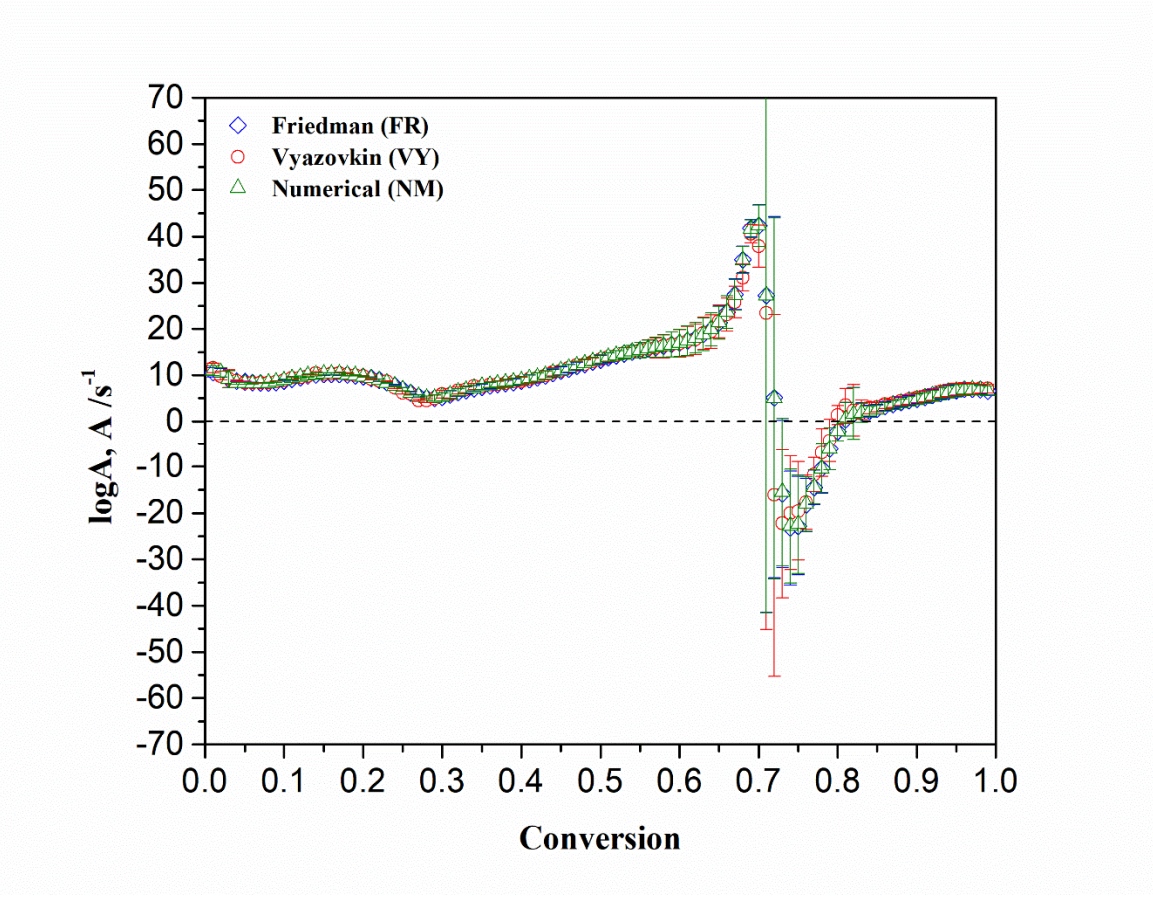

Figure S2. Multiconversional dependent logarithm of pre-exponential factors (*logA*(α)) obtained by Friedman (FR), Vyazovkin (VY) and Numerical (NM) methods, for thermo-oxidative degradation process of [4-(hydroxymethyl)phenoxymethyl] polystyrene resin (Scheme S1).

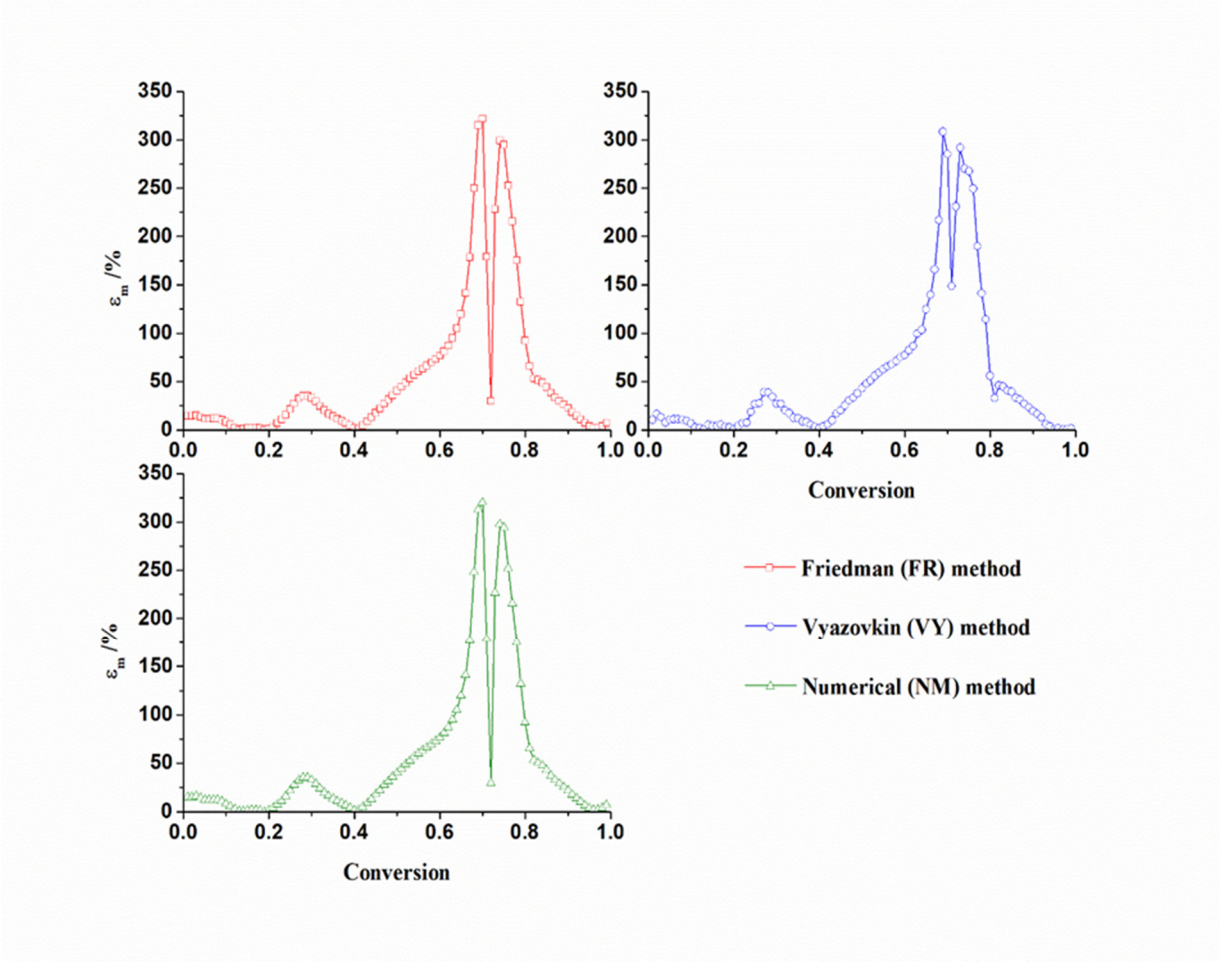

Figure S3. The deviation (ε_m) in the percentages of E_a values of FR, VY and NM methods to their mean E_a values (FR: $E_{a(mean)}$ = 142.498 kJ·mol^{-1}; VY: $E_{a(mean)}$ = 140.682 kJ·mol^{-1}; NM: $E_{a(mean)}$ = 143.023 kJ·mol^{-1}), for thermo-oxidative degradation process of [4-(hydroxymethyl)phenoxymethyl] polystyrene resin.

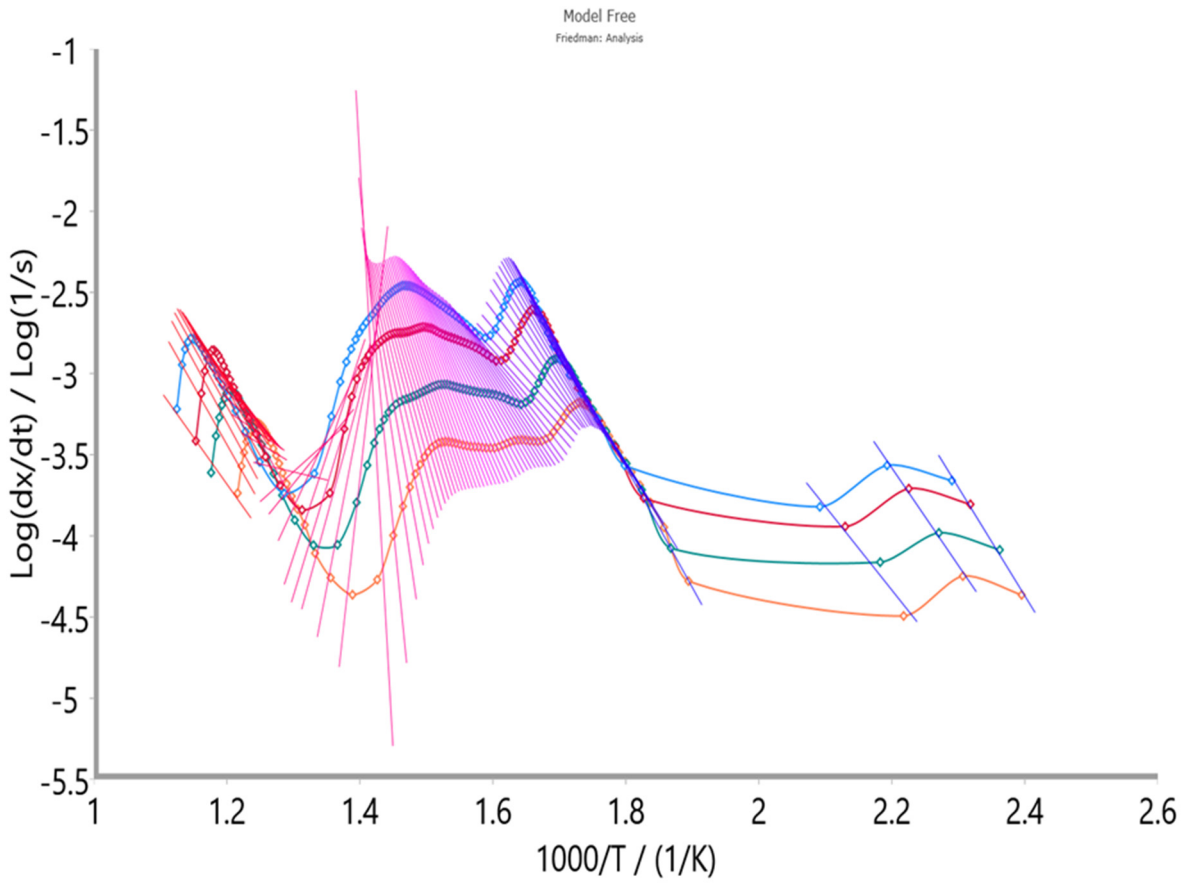

Figure S4. Friedman's (FR) isoconversional plots at every considered conversion value (with a step of $\Delta\alpha = 0.01$; an increase in the conversion (conversion is designated with "*x*" according to Kinetics Neo operational tool sheets, where $x \equiv \alpha$) goes from *right* to *left*), constructed for thermo-oxidative degradation process of [4-(hydroxymethyl)phenoxymethyl] polystyrene resin, at four different heating rates, β = 5, 10, 20 and 30 K/min (*orange* ◊: 5 K/min, *dark green* ◊: 10 K/min, *crimson red* ◊: 20 K/min, and *light blue* ◊: 30 K/min).

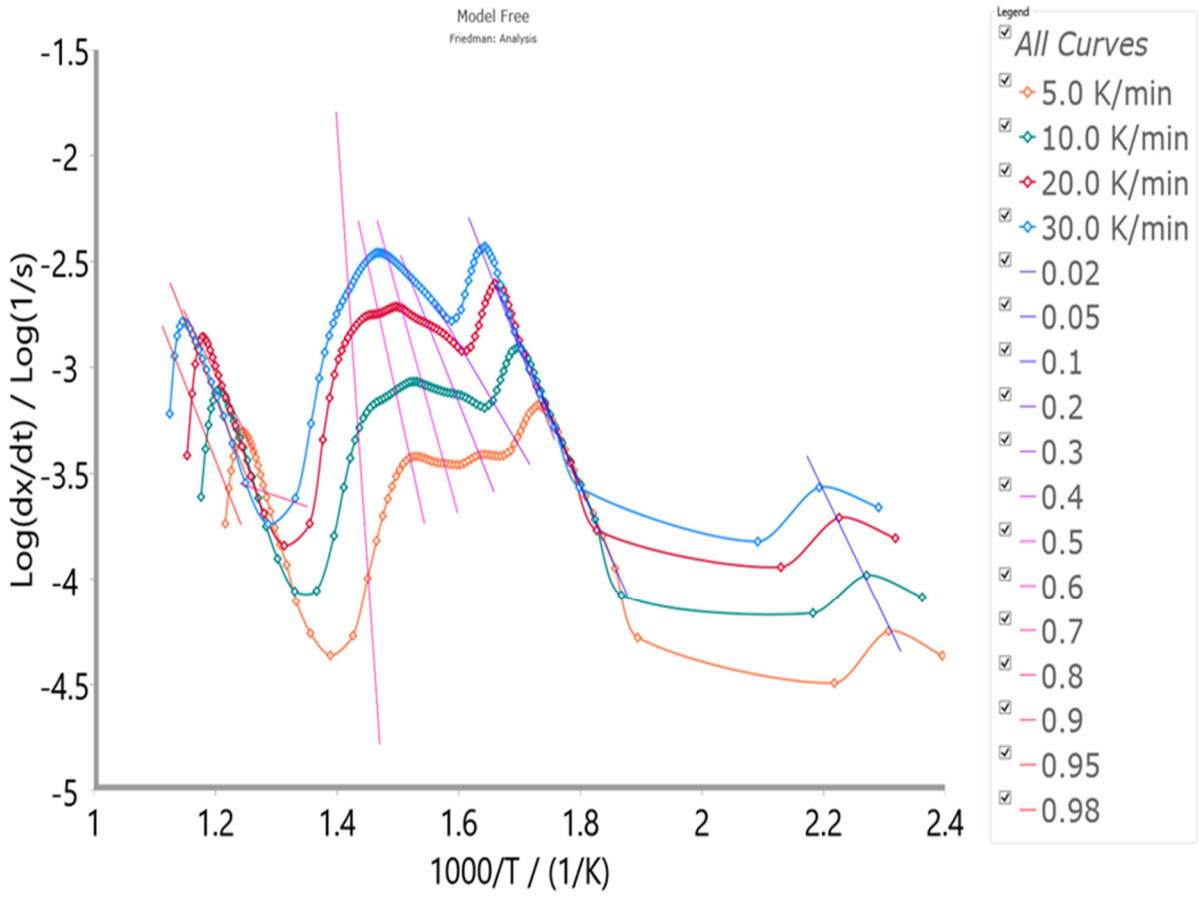

Figure S5. Friedman's (FR) isoconversional plots at the *selected* conversion values ($x \equiv \alpha$ = 0.02, 0.05, 0.1, 0.2, 0.3, 0.4, 0.5, 0.6, 0.7, 0.8, 0.9, 0.95, and 0.98) (conversion is designated with "*x*" according to Kinetics Neo operational tool sheets, where $x \equiv \alpha$), for thermo-oxidative degradation process of [4-(hydroxymethyl)phenoxymethyl] polystyrene resin, at four different heating rates.

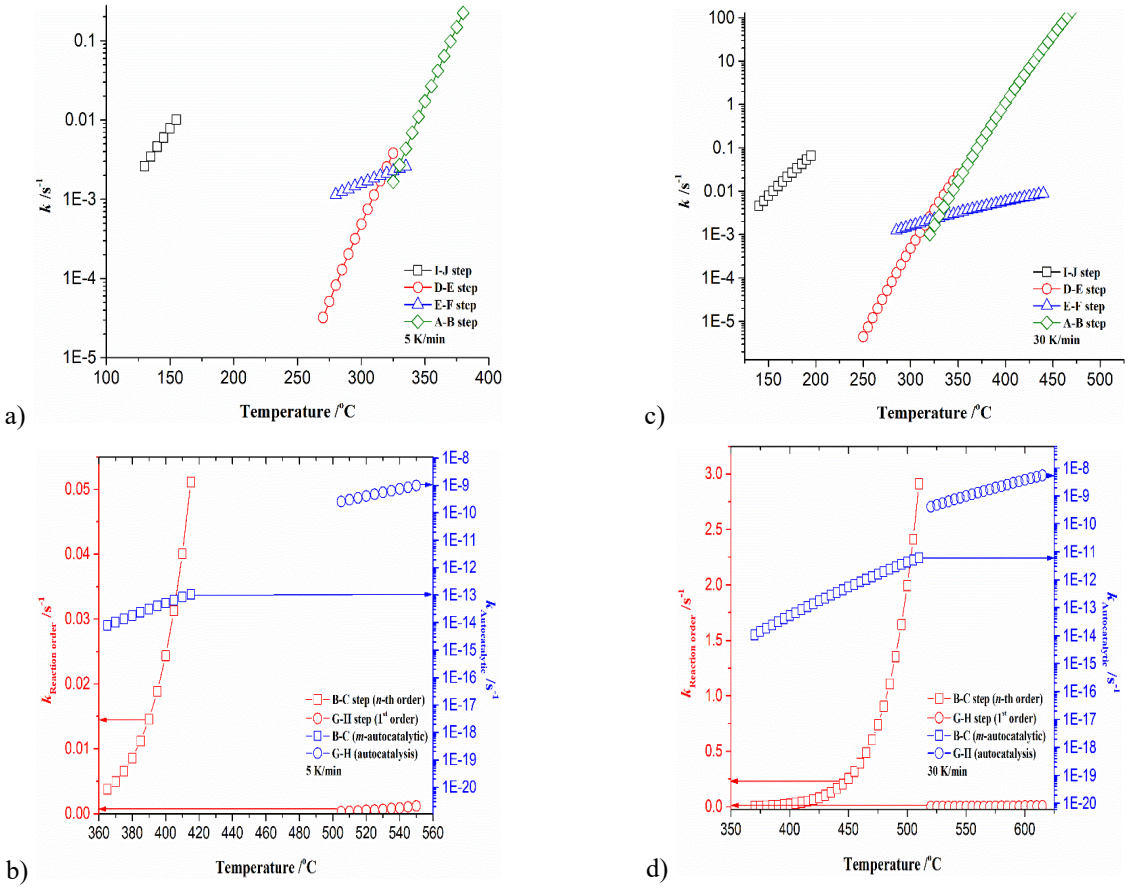

Figure S6. Rate constants behavior with the temperature, according to $k_{step}(T) = A_{step} \cdot exp(-E_{step}/RT_{(range)})$: **a)** for **I-J**, **D-E**, **E-F**, and **A-B** steps (5 K/min), **b)** for **B-C** step (*n*-th order and *m*-autocatalytic shares) and **G-H** step (for the first-order with autocatalysis share) (5 K/min), **c)** for **I-J**, **D-E**, **E-F**, and **A-B** steps (30 K/min), and **d)** for **B-C** step (*n*-th order and *m*-autocatalytic shares) and **G-H** step (for the first-order with autocatalysis share) (30 K/min).

a)

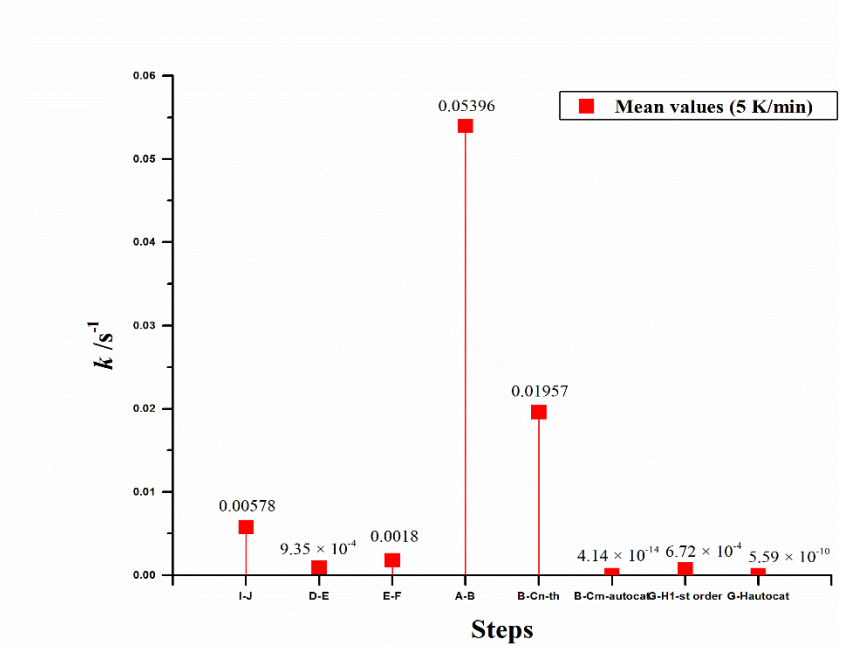

b)

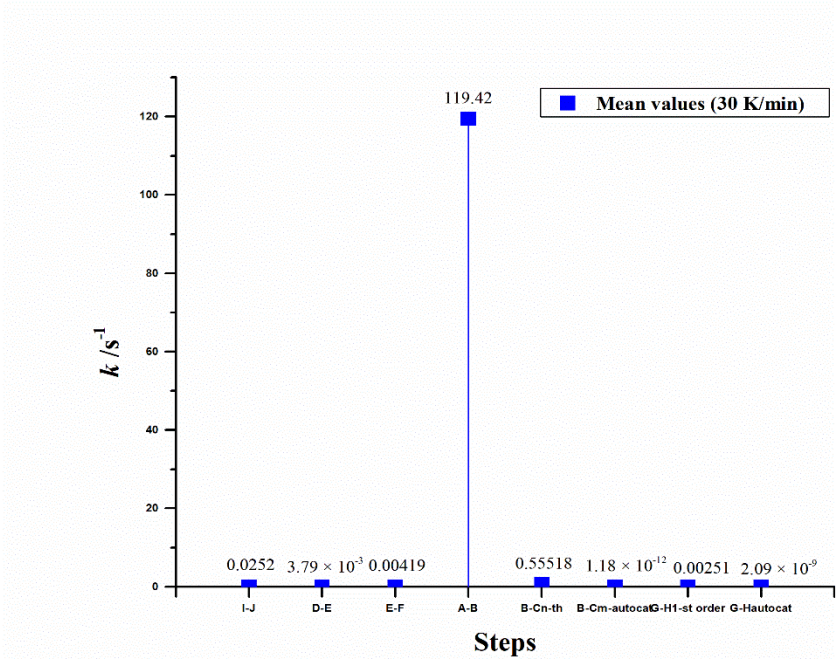

Figure S7. Mean rate constants for each individual reaction step in hx:, model, for: **a)** β = 5 K/min, and **b)** β = 30 K/min.

Table S3 Statistical analysis results (a statistical fit quality) for proposed hx:, model (obtained from model-based method) in the case of [4-(hydroxymethyl)phenoxymethyl] polystyrene resin degradation.

Method/Model	Fit to	R^2	Sum of dev. squares	Mean residual	Students coef. 95 %	F-test
hx:, model	TGA signal	0.99955	780.570	0.986	1.965	1.000

Table S4 Conditions for adiabatic 24 (h) predictions using Friedman (FR) (model-free) and hx:, (model-based) models, in terms of thermal safety of [4-(hydroxymethyl)phenoxymethyl] polystyrene resin.

Method/Model	**FR/hx:, Case 1**	**FR/hx:, Case 2**
Enthalpy (ΔH) ($J \cdot g^{-1}$)	120	120
Specific heat ($J \cdot g^{-1} \cdot K^{-1}$)	5	5
Phi (ϕ) (dimensionless)	1	1
TMR adiabatic (h)	24	24
Temp. initial (^{o}C)	30.97	91